# **RSC Chemical Biology**



# **REVIEW**

View Article Online



Cite this: RSC Chem. Biol., 2023,

Louise A. Stubbing, ab Jonathan G. Hubert, Joseph Bell-Tyrer, a Yann O. Hermant, Dab Sung Hyun Yang, Alice M. McSweeney, bc Geena M. McKenzie-Goldsmith, bc Vernon K. Ward, bc Daniel P. Furkert and Margaret A. Brimble \*\* \*\*ab

Pisoniviricetes class

Viral infections are one of the leading causes of acute morbidity in humans and much endeavour has been made by the synthetic community for the development of drugs to treat associated diseases. Peptide-based enzyme inhibitors, usually short sequences of three or four residues, are one of the classes of compounds currently under development for enhancement of their activity and pharmaceutical properties. This review reports the advances made in the design of inhibitors targeting the family of highly conserved viral proteases 3C/3CL<sup>pro</sup>, which play a key role in viral replication and present minimal homology with mammalian proteases. Particular focus is put on the reported development of P<sub>1</sub> glutamine isosteres to generate potent inhibitors mimicking the natural substrate sequence at the site of recognition.

P<sub>1</sub> Glutamine isosteres in the design of inhibitors

of 3C/3CL protease of human viruses of the

Received 25th May 2023, Accepted 19th June 2023

DOI: 10.1039/d3cb00075c

rsc.li/rsc-chembio

# Introduction

The Pisoniviricetes class encompasses a diverse range of positivesense single-stranded RNA viruses infecting eukaryotic organisms. Importantly to humans, this class includes the Picornaviridae, Coronaviridae and Caliciviridae families which represent some of the leading causes of acute morbidity in humans, and are among the most prevalent infectious agents. Picornaviruses are a large family of viruses, infecting both humans and animals, and their pathology ranges from mild infections such as the common cold and hepatitis A to more severe disease including meningitis and paralysis. In some instances viral infections by picornaviruses have been linked to autoimmune diseases such as myocarditis, diabetes, and multiple sclerosis.<sup>2-6</sup> Coronavirus infections also span a range of severity,<sup>2,7</sup> while caliciviruses are the leading cause of acute gastroenteritis but can have more severe symptoms in immunocompromised individuals.8 One of the unifying features of the Pisoniviricetes class is a highly structurally conserved cysteine protease belonging to the PA clan (proteases of mixed nucleophile,

superfamily A), commonly referred to as 3C<sup>pro</sup> (picornaviruses) or

which have characteristic folding of two equivalent β-barrels to form the binding pocket and a catalytic triad or dyad. 12-14 Substrate recognition is typically dictated by a hexapeptide sequence (P<sub>4</sub>-P<sub>3</sub>-P<sub>2</sub>-P<sub>1</sub>-P<sub>1</sub>'-P<sub>2</sub>'), each amino acid interacting with its corresponding binding site  $(S_x)$  of the protease enzyme (Fig. 1A). The scissile bond is between the  $P_1$ - $P_{1'}$  residues which are typically glutamine (Gln)-glycine (Gly), or Gln-other small amino acid. Though cleavage occurs less commonly, glutamic acid (Glu)-glycine (Gly) is another peptide bond of interest. 15,16 Crystal structures of 3Cpro and 3CLpro proteases along with substrate specificity studies have demonstrated subtle variation in the binding pockets and orientation of the catalytic triad/ dyad, however all are remarkably conserved to recognise glutamine at P<sub>1</sub> position. Specificity for P<sub>1</sub> glutamine is attributed to conserved histidine (His) residue located at the end of the S<sub>1</sub> binding pocket which form important hydrogen bonds with the glutamine side chain of the natural substrate. Due to the critical roles that 3C and 3CL<sup>pro</sup> play in viral replication and minimal homology with mammalian proteases, 3Cpro and 3CL<sup>pro</sup> have emerged as promising targets for drug

<sup>3</sup>CL<sup>pro</sup> (coronaviruses and caliciviruses, also known as M<sup>pro</sup>). 3C<sup>pro</sup> and 3CL<sup>pro</sup> enzymes play a critical role in viral replication, initially catalysing their autocleavage from the nascent polypeptide chain, before performing secondary cleavages leading to maturation of the viral replication machinery.9-11 3C<sup>pro</sup> and 3CL<sup>pro</sup> are chymotrypsin-like cysteine proteases,

<sup>&</sup>lt;sup>a</sup> School of Chemical Sciences, The University of Auckland, 23 Symonds Street and 3b Symonds Street, Auckland 1142, New Zealand. E-mail: m.brimble@auckland.ac.nz

<sup>&</sup>lt;sup>b</sup> Maurice Wilkins Centre for Molecular Biodiscovery, The University of Auckland, 3b Symonds Street, Auckland 1142, New Zealand

<sup>&</sup>lt;sup>c</sup> Department of Microbiology and Immunology, School of Biomedical Sciences, University of Otago, PO Box 56, 720 Cumberland Street, Dunedin 9054, New

Fig. 1 (A) Hexapeptide recognition sequence of 3C/3CL<sup>pro</sup>, where the scissile bond is located between  $P_1$  (Gln) and  $P_{1'}$ . (B) Typical inhibitor design targeting 3C/3CL<sup>pro</sup>.

development. A commonly employed approach in developing 3C/3CL<sup>pro</sup> inhibitors is to mimic the natural substrate sequence, replacing the scissile bond with an electrophilic warhead to capture the catalytic cysteine residue, either via a reversible or irreversible mechanism. Peptidyl inhibitors targeting 3C/3CL<sup>pro</sup> typically consist of a two to four peptide sequence (P<sub>4</sub>-P<sub>1</sub>), with glutamine occupying the P<sub>1</sub> position and an electrophilic "warhead" at P<sub>1</sub> while the N-terminal is protected (N-cap) (Fig. 1B).

Following this blueprint, a number of low micromolar inhibitors targeting 3C/3CL<sup>pro</sup> have been developed (representative examples, Fig. 2), 17-26 equipped with various electrophilic warheads demonstrating their effectiveness at trapping the catalytic cysteine residue. A drawback of employing a P<sub>1</sub> glutamine residue, however, is the high propensity for the amide side chain (Scheme 1A) to cyclise onto the electrophilic warhead, forming the hemiaminal tautomer (Scheme 1B). This reactivity has been observed with aldehyde, 17,27 α-haloketone, 23,28 and acyloxymethyl ketone<sup>25</sup> warheads containing P<sub>1</sub> glutamine or N-monoalkylated glutamine isosteres (see Section 1). Although the effects of tautomerisation to the hemiaminal are not clearly delineated, this is generally considered to be detrimental to antiviral activity while also causing complications during the chemical synthesis and purification. To avoid complications caused by the P<sub>1</sub> glutamine residue in the design of 3C/3CL<sup>pro</sup> inhibitors, incorporation of a glutamine isostere which binds specifically in the S<sub>1</sub> pocket while also preventing cyclisation onto the electrophilic warhead is desirable. This review reports the advances made in the design of inhibitors targeting viral 3C/3CL<sup>pro</sup> of human viruses in the Pisoniviricetes class and focusses on the reported development of P<sub>1</sub> glutamine isosteres.

#### Section 1. P<sub>1</sub> N-alkyl glutamine inhibitors

Early work in the development of P<sub>1</sub> glutamine isosteres focused on alkylation of the glutamine side chain amide to retard its nucleophilicity and prevent cyclisation onto the electrophilic warhead. Selected examples of inhibitors possessing a mono- or di-substituted amide side-chain at P1 position and equipped with various warhead units are presented in Fig. 3. Malcolm et al. explored tetrapeptide inhibitors with N,Ndimethyl-Gln at the P<sub>1</sub> position.<sup>29</sup>

This was proposed to prevent cyclisation onto the aldehyde warhead while also maintaining hydrogen bonding between the glutamine δ-carbonyl oxygen and His<sub>160</sub> of hepatitis A virus (HAV) 3C<sup>pro</sup>. <sup>12,29</sup> Inhibitor **1a** was based on the preferred substrate sequence and was found to be a reversible, slow binding inhibitor of HAV 3Cpro, while also being 50-fold less active against human rhinovirus (HRV) 3Cpro. Investigation of a series of P1 glutaminal inhibitors targeting HRV found N,Ndimethyl-Gln containing inhibitor 2b was  $\sim$  50-fold more active compared with the corresponding P<sub>1</sub> glutamine analogue 2a.<sup>27</sup> The low potency of 2a was postulated to be due to the propensity for cyclisation to the less active hemiaminal tautomer (see Scheme 1). A similar study was conducted investigating Michael acceptor tetrapeptides for anti-HRV activity. In this study however, unmodified glutamine inhibitor 3a was found to have superior activity (EC<sub>50</sub> =  $0.54 \mu M$ ) compared with both N-methyl-Gln 3b and N,N-dimethyl-Gln 3c containing analogues (EC<sub>50</sub> = 5.6  $\mu$ M and 4.0  $\mu$ M, respectively). The discrepancies in these studies likely arise from the propensity of the unprotected glutamine side chain to cyclise onto the aldehyde warhead, while Michael acceptors have not been observed to undergo cyclisation with the P<sub>1</sub> glutamine residue. <sup>18</sup> A related series of N-alkylated glutaminal inhibitors, cyclic tertiary amide exemplified by 4 were also shown to be effective in targeting norovirus (NV) 3CL<sup>pro</sup>.30

A glutamine N-alkylation strategy has also been employed to generate inhibitors equipped with an α-fluoromethyl ketone (FMK) warhead and targeting HAV31 and severe acute respiratory syndrome coronavirus (SARS-CoV)<sup>23,28,32</sup> Compound **1b** was found to inhibit HAV 3Cpro and displayed a second order rate constant of  $k_{\rm obs}/[I] = 3.3 \times 10^2 \ {\rm M}^{-1} \ {\rm s}^{-1.31}$  while N,Ndimethyl-Gln analogue 5a was shown to be a low micromolar inhibitor of SARS-CoV replication. 28 The analogous inhibitor 5b containing an unmodified Gln-FMK unit was found to be predominantly cyclised in solution (as observed by <sup>1</sup>H NMR) and 200-fold less active against SARS-CoV in a National Institute of Allergy and Infectious Diseases (NIAID) screen. An inhibitor containing an N-methyl-Gln-FMK unit 5c was on the other hand reported as active according to a personal communication in a footnote; however partial cyclisation in solution was observed by <sup>1</sup>H NMR and a series containing this N-methyl-Gln-FMK unit does not appear to have been pursued further. A series of glutamine-trifluoromethyl ketone inhibitors, represented by inhibitor 6a ( $K_i > 1000 \mu M$ ), were all found to be at least partially cyclised in solution (as determined by <sup>19</sup>F NMR in CDCl<sub>3</sub>), while some existed solely in their cyclic form. These exhibited only moderate anti-SARS-CoV activity23 while later work from the same laboratory showed N,N-dialkyl analogues **6b** and **6c** to have improved, albeit still low activity  $(K_i =$ 21.0  $\mu$ M, 34.1  $\mu$ M, respectively). 32

α-Ketophthalahydrazide warheads with P<sub>1</sub> N,N-dimethyl-Gln isosteres, as illustrated by 7, were investigated for anti-HAV

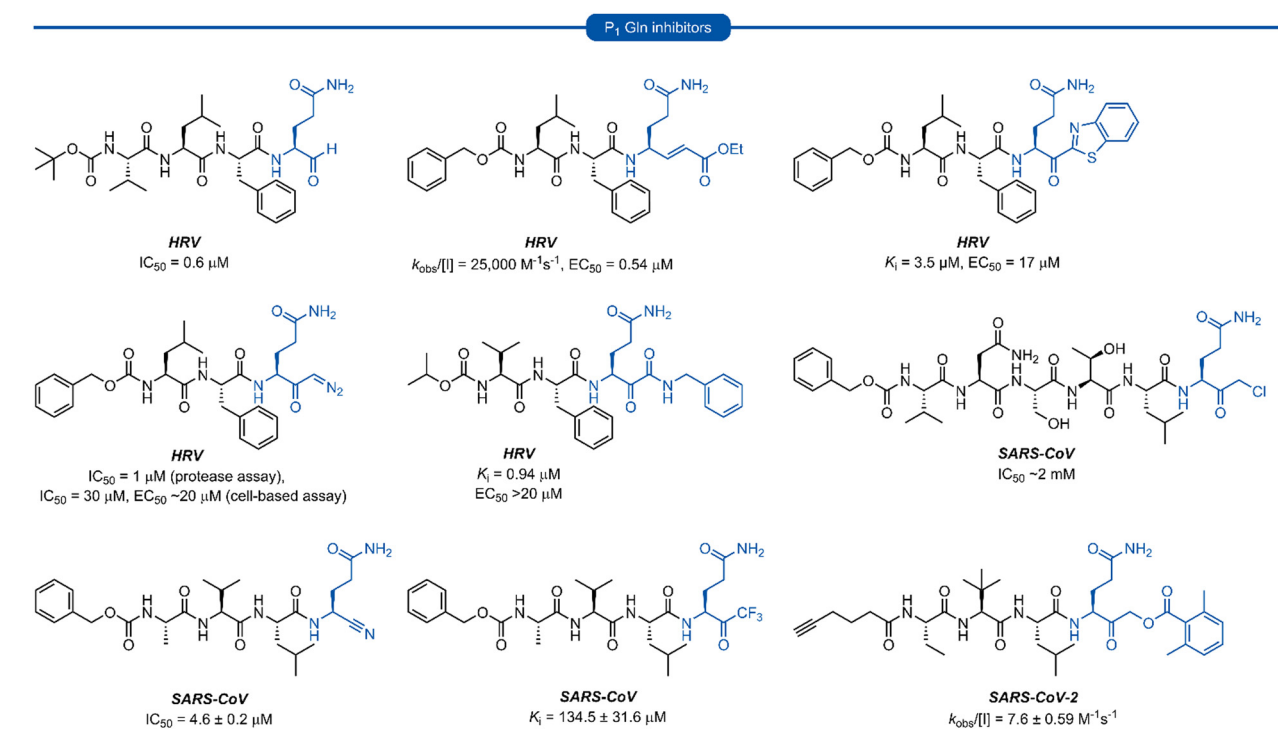
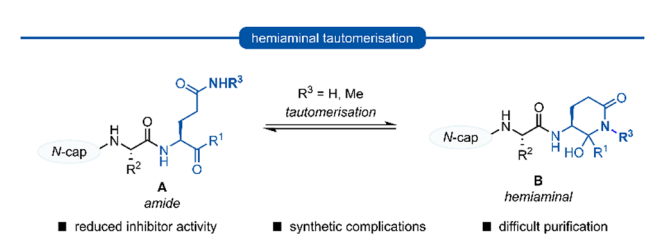


Fig. 2 Representative 3C/3CL<sup>pro</sup> inhibitors possessing a P<sub>1</sub> (L)-glutamine residue with various electrophilic warheads



Scheme 1 Generalised formation of hemiaminal B via tautomerisation of P<sub>1</sub> glutamine inhibitors A onto the electrophilic warhead

3C<sup>pro</sup> activity. 13,33 Intermolecular hydrogen bonding of the ketone and proximal hydrazide NH was postulated to restrict conformational mobility, thereby decreasing the entropic penalty upon binding, while also mimicking the P2' phenylalanine (Phe) of the natural substrate. 33 Compound 7 was found to be a competitive reversible inhibitor against HAV (IC<sub>50</sub> = 13  $\mu$ M), and no loss of activity was observed in the presence of a 100fold excess of dithiothreitol (DTT), indicating its stability to extracellular thiols.

#### Section 2. P1 methionine derived inhibitors

Methionine (Met) and its oxidised sulfoxide and sulfone derivatives have also been investigated as non-nucleophilic glutamine P<sub>1</sub> isosteres due to their ease of synthesis and H-bonding ability (Fig. 4). Methionine sulfone analogue 8a was found to be a good reversible inhibitor of HRV  $3C^{\text{pro}}$  ( $K_i = 0.47 \mu\text{M}$ ) and also displayed good antiviral activity in tissue culture assays (IC50 = 3.4 μM) with no observable cytotoxicity.<sup>34</sup> Additionally, inhibitor 8a was found to be more potent than inhibitors 8b and 8c containing a P<sub>1</sub> methionine or glutamine residue, respectively  $(IC_{50} = 9.7 \mu M \text{ and } IC_{50} = 42 \mu M).$ 

Similar observations were made in a separate study investigating aldehyde HRV 3Cpro inhibitors. Sulfoxide 9c displayed superior potency compared to analogue 9a containing an unmodified Gln residue (IC<sub>50</sub> = 0.005  $\mu$ M vs. 3.6  $\mu$ M), and was approximately equipotent to the N,N'-dimethyl-Gln analogue **9b.** The potency of sulfoxide **9c** was further supported by X-ray crystal structure data of the enzyme-inhibitor complex, which revealed the P<sub>1</sub> sulfoxide moiety fits snugly into the S<sub>1</sub> pocket and the H-bonding pattern of the active site His<sub>161</sub> and Thr<sub>142</sub> residues was analogous to that of the natural substrate.<sup>27</sup> The use of sulfoxide and sulfone P1 isosteres in conjunction with Michael acceptor warheads on the other hand has met with less success. Two separate studies both reported that peptidyl inhibitors of HRV 3C<sup>pro</sup> containing a P<sub>1</sub> sulfoxide **10a** or sulfone 10b and 11b residue showed a significant reduction in potency compared with their P<sub>1</sub> glutamine counterparts 3a and 11a, respectively. 19 Monopeptidyl aza-carboxamides, exemplified by 12a/b (For aza-backbone modifications, see Section 5) have also been investigated for anti HRV and HAV activity. P<sub>1</sub> sulfone 12b was found to have improved activity against HRV 3Cpro compared to N,N'-dimethyl-Gln analogue 12a. Conversely, 12a was found to exhibit slightly higher potency against HAV 3Cpro over 12b.<sup>35,36</sup>

#### Section 3. P<sub>1</sub> inhibitors derived from non-proteogenic amino acids

A number of P<sub>1</sub> glutamine isosteres derived from unnatural amino acids were investigated during the early development of

# P<sub>1</sub> N-alkyl Gln inhibitors HAV HRV HRV a: $R = NH_2$ , $K_i = 3.6 \mu M$ , $EC_{50} = 66 \mu M$ **a**: $\mathbf{R} = \mathbf{H}$ , $K_i = 4.2 \pm 0.8 \times 10^{-8} \,\mathrm{M}$ **a:** $R = NH_2$ , $k_{ODS}/[I] = 25000 \text{ M}^{-1}\text{s}^{-1}$ , $EC_{50} = 0.54 \mu\text{M}$ , **b**: $R = NMe_2$ , $K_i = 0.005 \mu M$ , $EC_{50} = 1.3 \mu M$ **b**: R = NHMe, $k_{obs}/[I] = 750 \text{ M}^{-1}\text{s}^{-1}$ , $EC_{50} = 5.6 \mu\text{M}$ **b**: $\mathbf{R} = \mathbf{CH_2F}$ , $k_{\text{obs}}/[\mathbf{I}] = 3.3 \times 10^2 \,\mathrm{M}^{-1} \mathrm{s}^{-1}$ c: $R = NMe_2$ , $k_{obs}/[I] = 60 \text{ M}^{-1}\text{s}^{-1}$ , $EC_{50} = 4.0 \text{ }\mu\text{M}$ NV SARS-CoV $K_i = 0.075 \mu M$ a: $R = NMe_2$ , $EC_{50} = 2.4 - 3.6 \mu M$ (across 3 cell lines) b: R = NH<sub>2</sub>, 200-fold less active in NIAID screen c: R = NHMe, reported as active 6a 6b SARS-CoV SARS-CoV SARS-CoV $K_i$ = 21.0 ± 4.3 $\mu$ M $K_i = 34.1 \pm 4.1 \, \mu M$ $K_i = >1000 \text{ uM}$ HAV

Fig. 3 Representative examples of P<sub>1</sub> N-alkyl-Gln inhibitors targeting 3C/3CL<sup>pro</sup>.

 $IC_{50} = 13 \mu M$ 

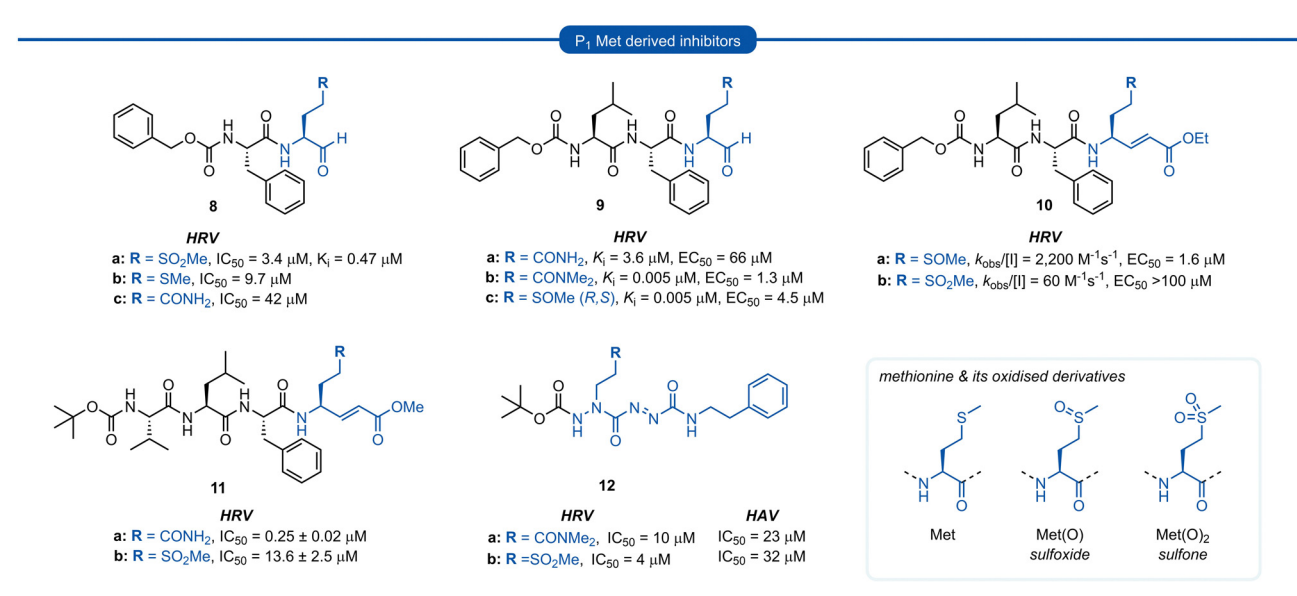
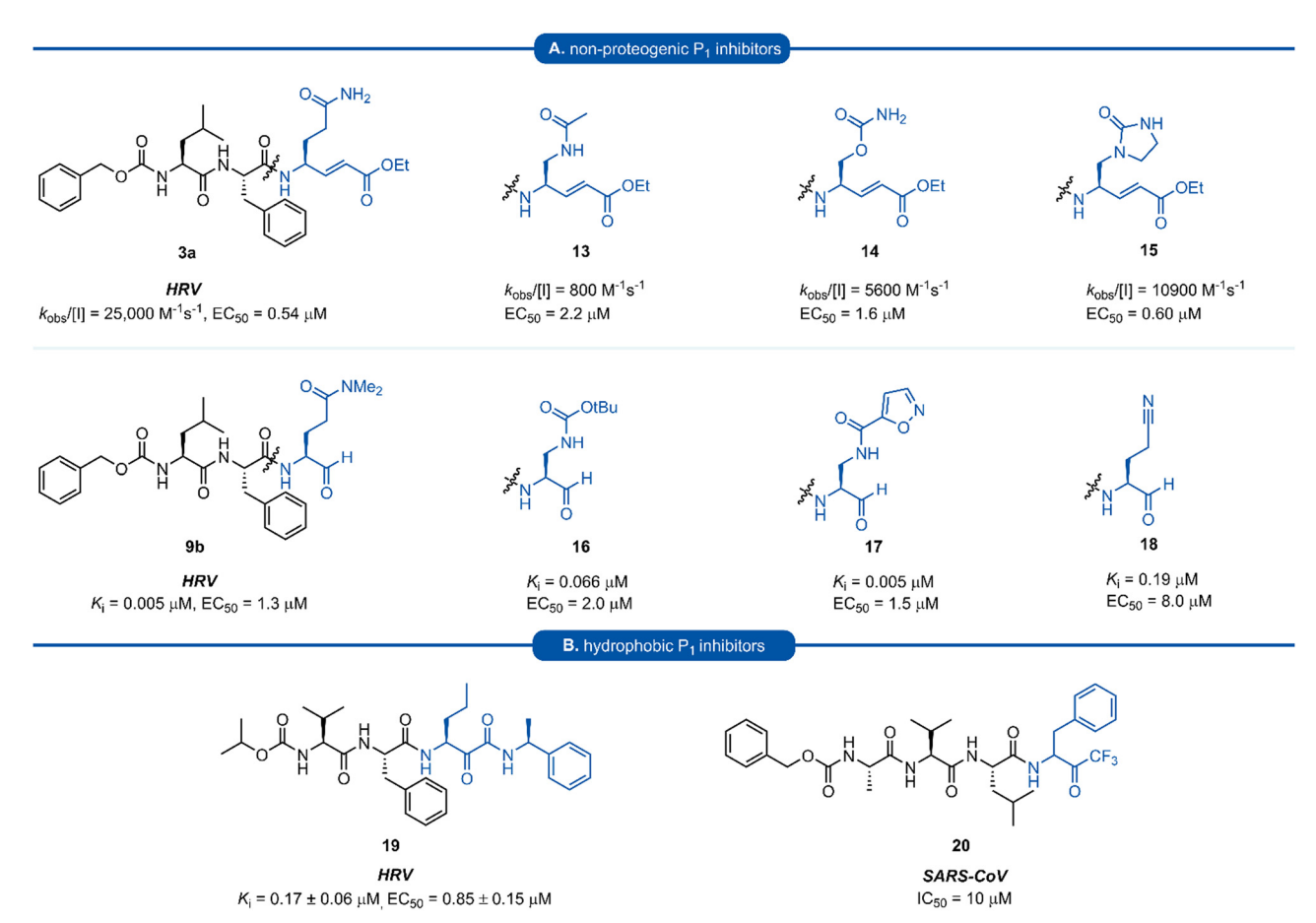


Fig. 4 Representative examples of P<sub>1</sub> Met derived inhibitors and their P<sub>1</sub> Gln/N-alkyl-Gln analogues targeting 3C/3CL<sup>pro</sup>.

3C/3CL<sup>pro</sup> inhibitors. Most notably, publications by Dragovich et al. and Webber et al. explored a diverse array of P1 derivatives including glutamine related P1 substrates (Section 1) and nonglutamine derived P1 residues such as sulfones/sulfoxides (Section 2), as well as a number of glutamine isosteres (representative examples, Fig. 5A). During these studies however, none of these analogues 13-15 or 16-18 showed increased potency over inhibitors containing the unmodified side chain



(A) Inhibitors targeting 3C/3CL<sup>pro</sup> containing non-proteogenic P<sub>1</sub> isosteres. (B) Hydrophobic P<sub>1</sub> residue inhibitors targeting 3C/3CL<sup>pro</sup>

 $3a^{19}$  or the *N*,*N'*-dimethyl-Gln  $9b^{27}$  derivatives, respectively. Alternatively, peptidyl inhibitors bearing a hydrophobic amino acid in the P<sub>1</sub> position have also been investigated (Fig. 5B). The substitution of P<sub>1</sub> glutamine with non-nucleophilic residues circumvented synthetic complications caused by the reactivity of the electrophilic warhead. Representative examples 19 and 20 possess a norvaline (Nva) or phenylalanine hydrophobic amino acid at the P<sub>1</sub> position, respectively. Norvaline P<sub>1</sub> tetrapeptide inhibitor 19 was found to have low micromolar activity against HRV  $3C^{pro}$  ( $K_i = 0.17$ ) and also having good activity in tissue culture (EC<sub>50</sub> = 0.85  $\mu$ M), <sup>24</sup> while P<sub>1</sub>-phenylalanine inhibitor 20 was found to exhibit moderate time-dependent activity against SARS-CoV 3CL<sup>pro</sup> (IC<sub>50</sub> = 10 µM).<sup>37</sup> A recent development in the inhibitor design has been made using self-masked aldehyde inhibitors (SMAIs) methodology for targeting 3CL protease.<sup>38</sup> Originally developed by Meek and co-workers to target cruzain, SMAIs was then applied to the development of SARS-CoV-2 inhibitor 21.39 SMAIs methodology is designed to mask the reactive aldehyde warhead through the spontaneous formation of a δ-lactol via nucleophilic attack by the P<sub>1</sub> 2-pyridone side-chain on the aldehyde warhead, which would closely mimic the  $\gamma$ -lactam  $P_1$  moiety that is now commonly employed in the design of 3C/3CL protease inhibitors (see Section 7). Upon binding to the protease active site, acid catalysed ring-opening by an acidic residue, revealing the

reactive aldehyde warhead, which captures the cysteine residue to afford the enzyme-bound moiety (Scheme 2).

Formation of the lactol moiety was confirmed by NMR in organic solvents, however, unambiguous confirmation of the major species in aqueous solutions has not been made.<sup>38</sup> Compound 21 was found to be a competent inhibitor of SARS-CoV-2 with EC<sub>50</sub> value of 5 μM. A high-resolution X-ray crystal structure of 21 bound in the active site of SARS-CoV-2 3CL<sup>pro</sup> confirmed the formation of the anticipated hemithioacetal between the aldehyde group and Cys145, thereby confirming the inhibitor's mechanism of action. The P<sub>1</sub> 2-pyridone residue also establishes the expected H-bonding pattern, with the 2-pyridone carbonyl group accepting H-bonding from His<sub>163</sub> and Ser<sub>144</sub> while the amide proton donates an H-bond to Glu<sub>166</sub> and Phe<sub>140</sub>.38

#### Section 4. P<sub>1</sub> histidine inhibitors

During work towards the development of SARS-CoV 3CL<sup>pro</sup> inhibitors, investigations into the substrate preference for SARS-CoV 3CL<sup>pro</sup> via positional scanning of synthetic recombinant libraries based on the 7-amino-4-carbamoyl-coumarin (ACC) fluorogenic leaving group were undertaken.

A surprising preference for histidine at P1 was revealed which was further confirmed by synthesising single substrates and comparing their kinetic constraints (Fig. 6).40 Early investigations Review

Scheme 2 Putative mechanism of reversible covalent inhibition of a cysteine protease by SMAIs.

P<sub>1</sub> His inhibitors

P<sub>1</sub> His inhibitors

P<sub>1</sub> His inhibitors

P<sub>1</sub> His inhibitors

P<sub>2</sub> His inhibitors

Aza-decaline unit substitution at P<sub>2</sub> position

$$C_{50} = 65 \text{ nM}$$

Aza-decaline unit substitution at P<sub>2</sub> position

 $C_{50} = 26 \text{ µM}$ 

Aza-decaline unit substitution at P<sub>2</sub> position

 $C_{50} = 26 \text{ µM}$ 

Aza-decaline unit substitution at P<sub>2</sub> position

 $C_{50} = 260 \text{ µM}$ 

Representative examples of P<sub>1</sub> His inhibitors targeting SARS-CoV 3CL<sup>pro</sup>

of histidine P<sub>1</sub> analogues for anti SARS-CoV activity initially led to the discovery of the potent tetrapeptide inhibitor 22 ( $IC_{50}$  = 65 nM). 41 Analysis of the binding pocket of the inhibitor 22bound X-ray crystal structure showed that the cyclohexyl ring of the P<sub>2</sub> cyclohexylalanine (Cha) was proximal to the α-nitrogen of the corresponding amino acid residue. A novel decahydroisoquinoline inhibitor scaffold was designed by introduction of a methyl linker between the P<sub>2</sub> cyclohexyl ring and the P<sub>2</sub> backbone nitrogen and a peptide chain extending off the 3-position of the ring system of compound 23. Although compound 23 represents a novel class of 3CL<sup>pro</sup> inhibitors, improved potency against SARS-CoV 3CL<sup>pro</sup> compared with its linear predecessor 22, was not achieved. 42-44 Histidine P<sub>1</sub> residues were also employed by Hayashi et al. against 3CLpro of SARS-CoV using α-keto-thiazole warheads 24, however, these did not show superior activity to analogous P1 lactam inhibitors (see Section 7) and were not further explored.45

#### Section 5. P<sub>1</sub> aza-glutamine inhibitors

Azapeptides are peptide chains where one of the amino acid residues are replaced by a semicarbazide which conformationally restricts the peptide, bending the amino acid away from the natural linear geometry. Incorporation of semicarbazides into peptidyl inhibitor manifolds has been shown to improve

activity and selectivity while also showing improved pharmacokinetic properties such as metabolic stability and duration of action. 46 The success of aza-backbone modifications at the P1 position of papain inhibitors initially led to their incorporation in the design of inhibitors for the closely related 3C/3CL<sup>pro</sup> (Fig. 7).47,48 Norbeck et al. developed P1 aza-glutamine bromomethylketone 25 for anti-HRV activity as a time-dependent irreversible inhibitor ( $k_{\text{inact}}/K_{\text{inact}} = 23\,400\,\text{ M}^{-1}\,\text{s}^{-1}$ ). In a separate study, a series of aza-glutamine inhibitors such as 26 were found to have moderate activity against both HRV and HAV  $3C^{\text{pro}}$  (IC<sub>50</sub> = 12  $\mu$ M and IC<sub>50</sub> = 10  $\mu$ M) respectively.<sup>35</sup> Although a number of P1 aza-glutamine inhibitors have been investigated, generally only moderate potency has been achieved against HRV and HAV. 48,51 P1 aza-glutamine inhibitors have also been developed against SARS-CoV. Notably, James et al. demonstrated through X-ray crystal structure elucidation that aza-glutamine epoxide 27 irreversibly binds *via* an induced-fit model. 52,53 Müller and co-workers have also developed a potent inhibitor of 3CL<sup>pro</sup> SARS CoV-2 containing a N-methyl-azanitrile warhead unit 28 ( $K_i = 24 \text{ nM}$ ).

#### Section 6. P<sub>1</sub> Gln macrocyclic inhibitors

Macrocyclic inhibitors have been shown to display improved properties over their acyclic counterparts for the inhibition of

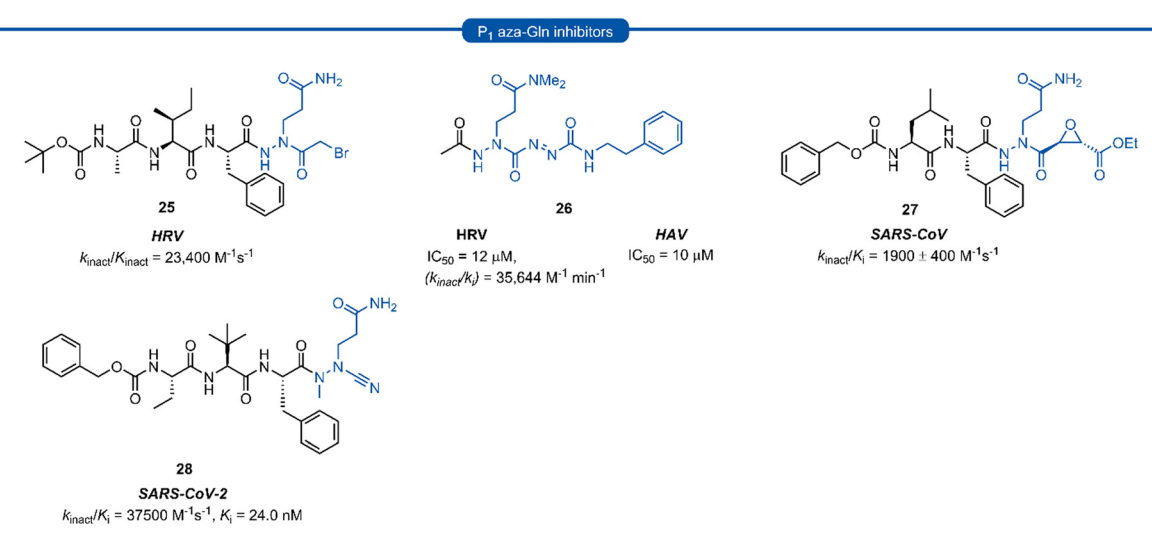
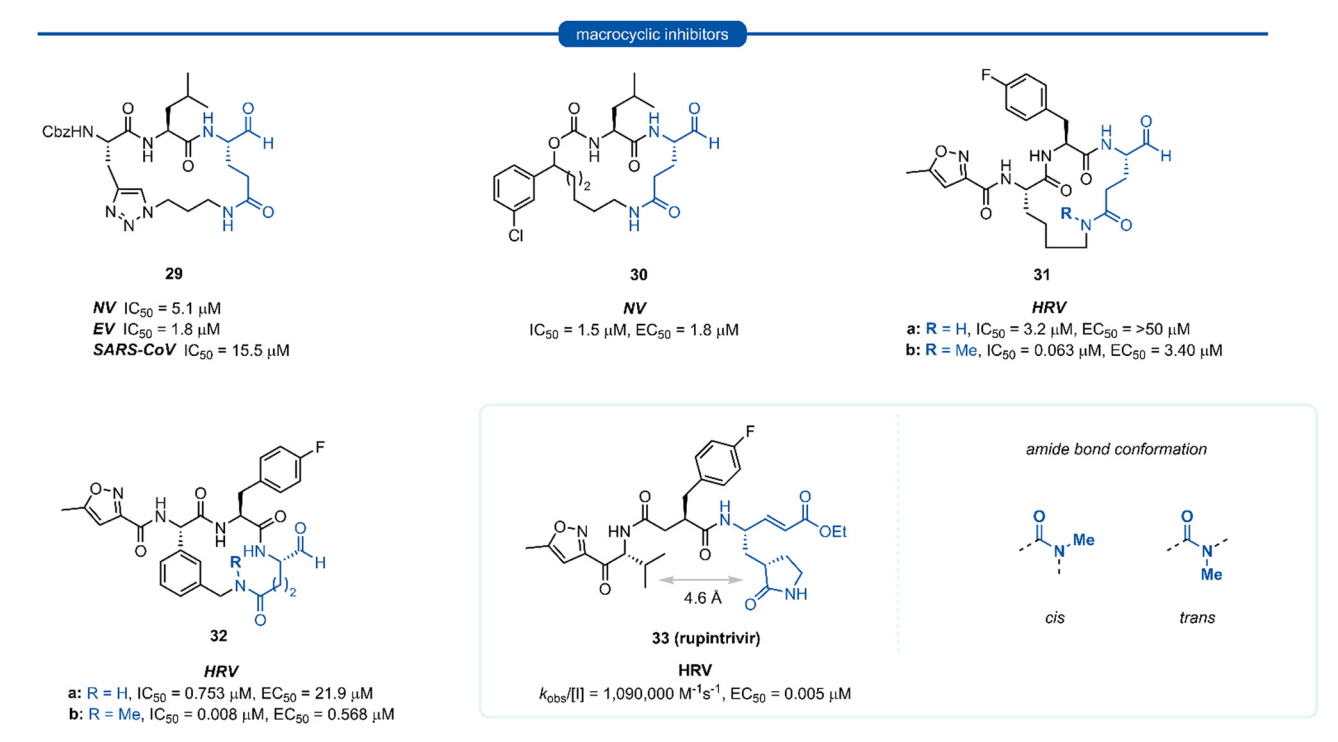


Fig. 7 Representative examples of P<sub>1</sub> aza-Gln inhibitors targeting 3C/3CL<sup>pro</sup>

protease enzymes. Protease enzymes recognise their ligands in a β-strand conformation, and macrocyclization can help facilitate the backbone hydrogen bonding pattern of peptide inhibitors to mimic that of an extended antiparallel  $\beta$ -sheet of the natural substrate. 55-57 Macrocyclization may also increase the structural rigidity of peptide-based inhibitors, restricting the conformational interchange and thereby enhancing the affinity for the receptor by reducing the loss of entropy upon binding, as well as exhibiting improved receptor selectivity and favourable drug-like characteristics including increased cell permeability and proteolytic stability. 55,58-60 The first investigations into macrocyclic 3C<sup>pro</sup> and 3CL<sup>pro</sup> inhibitors arose from analysis of the crystal structure of inhibitors bound to HRV 3C<sup>pro</sup>, revealing close spatial proximity between P<sub>1</sub> and P<sub>3</sub> side-chains. Modelling studies yielded tripeptidyl macrocyclic inhibitor 29, where a triazole-containing linker adjoined the P<sub>1</sub> and P<sub>3</sub> residues (Fig. 8). The inhibitor activity was evaluated against norovirus, enterovirus and SARS-CoV, and in all cases 29 was found to inhibit the protease in the low micromolar range.<sup>61</sup> Further investigation showed poor correlation between 3CL<sup>pro</sup> enzyme inhibition assays (IC50) and inhibition of norovirus replication in a cell-based replicon system assays (EC50) for 29



Representative examples of macrocyclic lactam inhibitors containing a P<sub>1</sub> Gln residue.

and derivatives thereof. 62 This result indicates that compounds such as 29 likely suffer from poor cellular permeability due to the triazole ring increasing the polar surface area. An X-ray crystal structure of NV 3CL<sup>pro</sup> with bound inhibitor 29 revealed the expected antiparallel β-sheet backbone binding conformation, and the tetrahedral adduct between the aldehyde warhead and  $Cys_{139}$  residue was also present. It was noted however, that binding induced suboptimal structural changes of the protease binding pocket and more importantly, the S<sub>1</sub> pocket, resulting in loss of the key Thr<sub>134</sub> and His<sub>157</sub> H-bonds to P<sub>1</sub> Gln and thus maximal binding efficiency was not obtained. 62,63 Further publications explored related macrocyclic inhibitors with alkyl linkers which generally gave increased cell permeability, with inhibitor 30 found to have good activity in both enzyme and cell-based assays. Co-crystallisation of 30 and NV 3Cpro showed the expected backbone H-bonding pattern indicating the expected bonding orientation. The key H-bonding interaction between the P<sub>1</sub> amide of 30 and His<sub>157</sub> and Thr<sub>134</sub> of NV 3C<sup>pro</sup> however was again absent; instead, a new H-bond between the oxygen of the tetrahedral thioacetal adduct and Pro136 was evident.64 Rupintrivir 33 (AG-7088), a potent anti-rhinoviral agent that became the subject of extensive preclinical and clinical investigation, was used as a scaffold for macrocyclic inhibitors, with the goal of improving rupintrivir's pharmacokinetic properties.<sup>65</sup> The crystal structure of rupintrivir/HRV2 3C<sup>pro</sup> showed only 4.6 Å between the P<sub>1</sub> and P<sub>3</sub> side chains, providing an opportunity for the introduction of a macrocyclic linkage.

The resulting macrocycle 31a was tested against HRV 3Cpro and showed decreased potency compared to rupintrivir  $(EC_{50} > 50 \,\mu\text{M})$  in HeLa cells infection model, albeit conserving moderate protease inhibition activity with IC<sub>50</sub> values in the low micromolar range (IC<sub>50</sub> =  $3.2 \mu M$ ). Modelling of the macrocyclic peptide in the binding pocket predicted the glutamine-derived amide bond was required to be in the cis conformation for efficient binding. Despite the cis conformation being higher energy, methylation of the amide nitrogen allows increased population of the cis conformer. Inhibitor 31b containing an N-methyl moiety showed a 50-fold increase in potency against HRV  $3C^{pro}$  (IC<sub>50</sub> = 0.063  $\mu$ M) despite losing an H-bonding interaction between the P<sub>1</sub> amide proton and backbone carbonyl of Thr<sub>142</sub>. Alternatively, incorporation of a phenyl ring into the macrocyclic linkage gave inhibitor 32a (IC<sub>50</sub> =  $0.753 \mu M$ ), which displayed a 4-fold increase in activity over 31a. Additional incorporation of the N-methyl moiety afforded 32b and further increased the activity by 100-fold (IC<sub>50</sub> = 0.008  $\mu$ M).

#### Section 7. P<sub>1</sub> lactam inhibitors

Pioneering work by Dragovich and co-workers first led to the use of  $\gamma$ -lactams as  $P_1$  glutamine isosteres in a series of publications developing tripeptide inhibitors of HRV  $3C^{\rm pro}$ .  $^{18,19,66,67}$  Early investigations (see Sections 3 and 4) found that none of the  $P_1$  non-glutamine inhibitors showed improved potency over the inhibitor containing an unmodified glutamine side chain 3a (Fig. 9A). Inspection of the X-ray crystal structure of 3a bound to HRV  $3C^{\rm pro}$  revealed that while the  $P_1$  trans amide

proton is engaged in a H-bond to the backbone carbonyl of  $\operatorname{Thr}_{142}$ , the *cis* amide proton is solvent exposed, providing a vector for further optimisation of the  $P_1$  side chain. *N*-Monomethyl inhibitor **3b** displayed significantly weaker protease inhibition, presumably due to the amide preferentially adopting a *trans* conformation, interrupting the key  $P_1$  amide proton-Thr<sub>142</sub> H-bond (Fig. 9A). In order to lock in the desired *cis* amide conformation, an (*S*)- $\gamma$ -lactam was incorporated into the  $P_1$  side chain.

The resulting tripeptide 34a displayed a remarkable increase in protease inhibition activity against HRV 3Cpro as well as submicromolar antiviral activity in cell culture.<sup>67</sup> The combination of this newly optimised P<sub>1</sub> side chain with favourable P<sub>2</sub>-P<sub>4</sub> modifications discovered in related work gave rise to rupintrivir 33 (AG-7088). During the initial investigation into P<sub>1</sub> lactambased glutamine isosteres, it was found that while a (S)-δlactam moiety 34b was equally effective as the (S)- $\gamma$ -lactam 34a, switching the stereochemistry of the lactam ring 34c or replacing the lactam moiety with a 5-membered cyclic urea 34d resulted in a significant reduction in activity (Fig. 9B).<sup>67</sup> Following the work of Dragovich et al. and guided by crystal structure studies revealing the high degree of structural homology among 3C<sup>pro</sup> and 3CL<sup>pro</sup> enzymes, P<sub>1</sub> (S)-lactam isosteres have been integrated into the design of numerous inhibitors targeting 3C/3CL<sup>pro</sup>. The first example outside of the preliminary work on HRV protease was for the development of inhibitors of hepatitis A virus (HAV) 3Cpro. From a small series of compounds bearing an α-ketophthalahydrazide, compound 35 proved to be the most effective ( $IC_{50} = 1.6 \mu M$ ). Representative examples of 3C/3CL<sup>pro</sup> inhibitors bearing a P<sub>1</sub> (S)-lactam isostere are shown in Fig. 10, showcasing the compatibility of the P<sub>1</sub> (S)-lactam with a range of electrophilic warhead functionalities. The (S)-lactam P1 unit has been shown to be effective in targeting numerous viral 3C/3CL<sup>pro</sup> including compounds **36–38** for enterovirus, <sup>69–74</sup> **39** for norovirus, <sup>75–79</sup> **40–41** for SARS-CoV, 32,45,80-89 **42** for MERS-CoV, 90-92 and **43-51** for SARS-CoV-2 (Fig. 11). A handful of inhibitors demonstrating broad spectrum activity have also been developed. 93-96 As represented in Fig. 10, 3C/3CL<sup>pro</sup> inhibitors typically employ a (S)- $\gamma$ -lactam  $P_1$  isostere, however enterovirus has been shown to prefer the (S)- $\delta$ -lactam isostere at the P<sub>1</sub> position. This was first demonstrated through docking studies of EV71 3Cpro, revealing the δ-lactam had shorter H-bond distances with  $His_{161}$  and  $Thr_{142}$  compared to the  $\gamma$ -lactam, while also adopting a preferable binding orientation in the S<sub>1</sub> pocket.<sup>70,71</sup> This model was validated through the design of inhibitor 36c, which was 7–10 fold more active than the corresponding  $\gamma$ -lactam 36b. In a separate study, screening of a compound library revealed compound 37 containing a chiral cyanohydrin warhead. 72 Each epimer was tested separately and exhibited good activity against EV71 with little effect of the warhead stereochemistry on the potency of the inhibitor. The same library screening also revealed an inhibitor scaffold analogous to that of 37 with an aldehyde warhead 38, to be the most potent compound tested against EV71 in both 3Cpro protease inhibition assay and human rhabdomyosarcoma cells viral infection model.<sup>70-72</sup>

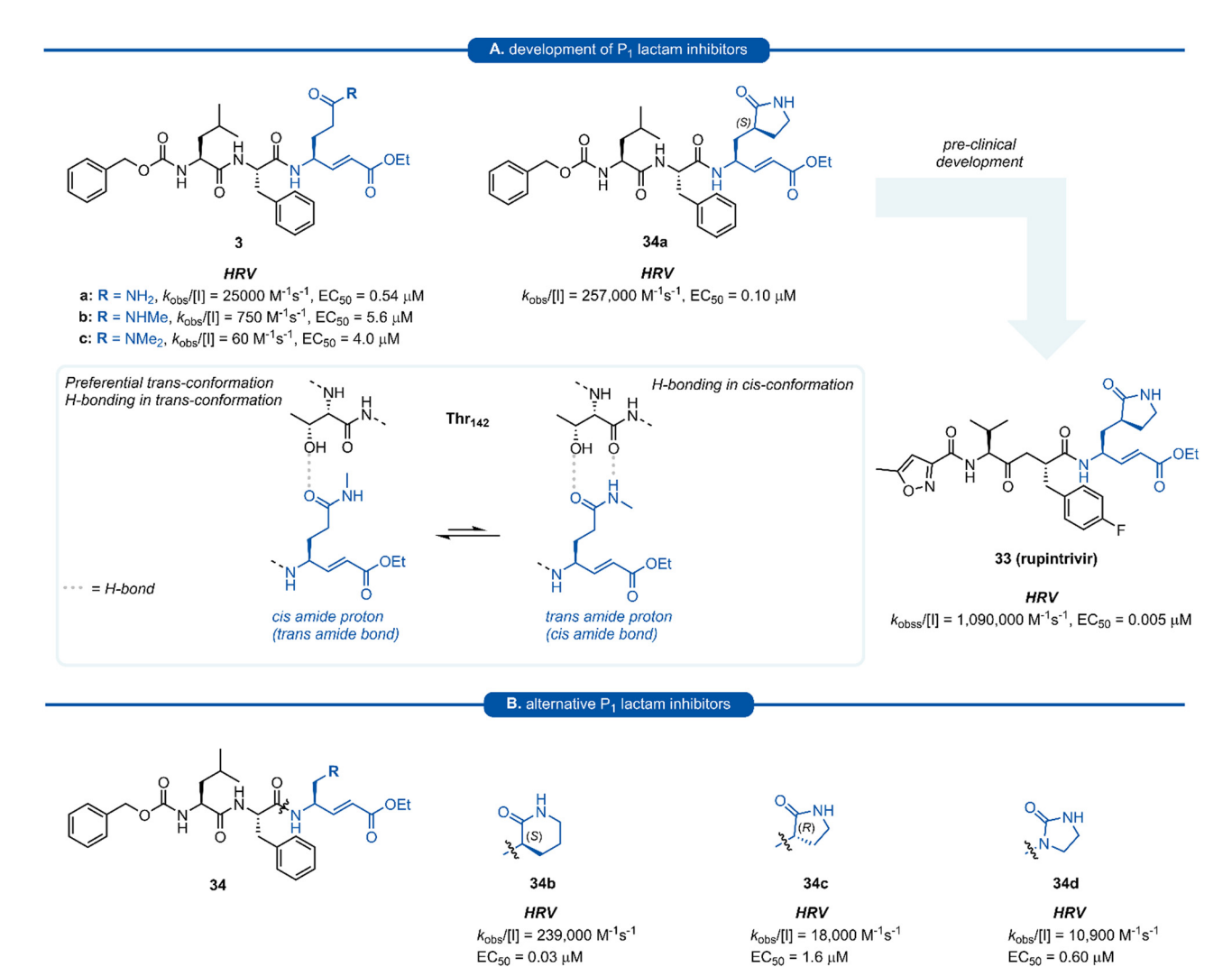
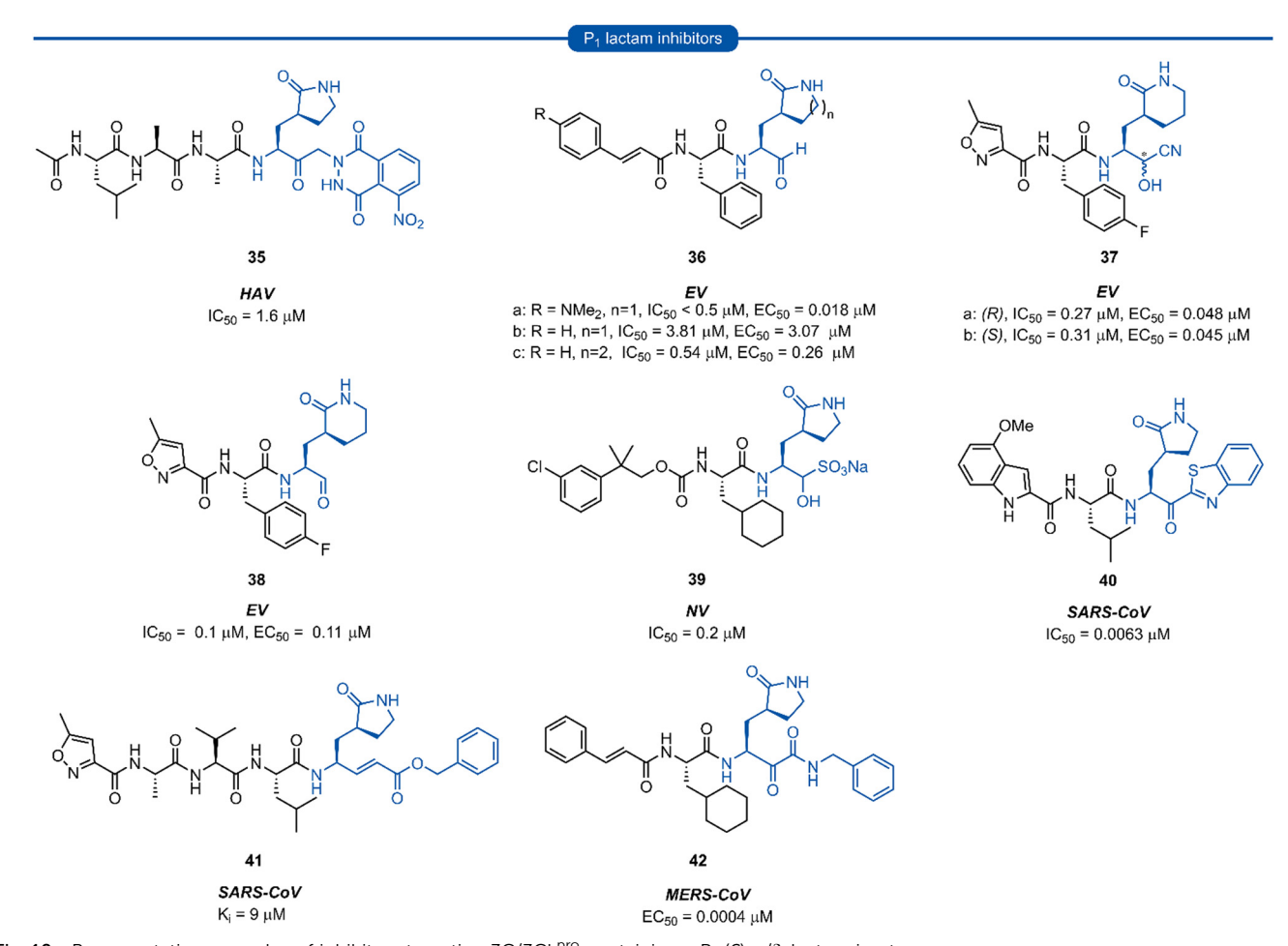


Fig. 9 (A) Development of HRV inhibitors possessing a  $P_1$  (S)- $\gamma$ -lactam moiety. (B) Alternative  $P_1$  lactam isosteres.

Since the SARS-CoV-2 outbreak in 2019, new inhibitors of the main protease 3CL<sup>pro</sup> (aka M<sup>pro</sup>, Nsp5) have almost exclusively been developed using  $P_1$  (S)- $\gamma$ -lactam isostere. In early work, it was realised that a high degree of homology existed between 3CL pro of SARS-CoV and SARS-CoV-2.97 In addition to their 96% sequence identity, X-ray crystal data has demonstrated there to be a high structural similarity between SARS-CoV and SARS-CoV-2 3CL<sup>pro</sup> with a root mean square deviation of 0.53 Å across all Cα positions. 98 This suggested that structural features from known coronaviral protease inhibitors are likely to be effective when incorporated into the design of SARS-CoV-2 3CL<sup>pro</sup> inhibitors. This was demonstrated in an early report by Hilgenfeld and co-workers in the development of  $\alpha$ -ketoamide inhibitor 43 from known inhibitor 42. The (S)- $\gamma$ lactam moiety was found to occupy the 3CL<sup>pro</sup> S<sub>1</sub> pocket, with the crystal structure of SARS-CoV-2 3CL<sup>pro</sup> with 43 highlighting the crucial H-bonding between the lactam carbonyl oxygen with His<sub>163</sub> side-chain imidazole, and the lactam nitrogen forming a three-centred hydrogen bond with Phe<sub>140</sub> and Glu<sub>166</sub>. 98 Various electrophilic warhead moieties have been demonstrated as

effective in combination with a  $P_1(S)$ - $\gamma$ -lactam group targeting SARS-CoV-2 3CL<sup>pro</sup>. Dipeptides bearing a heterocyclic acyloxymethylketone warhead were shown to be excellent irreversible inhibitors of SARS-CoV-2 3CL<sup>pro</sup>, exemplified by 44.99 Compound 44 also exhibited excellent plasma stability, glutathione stability, and selectivity over human proteases cathepsin B and cathepsin S. Inhibitor 45, which possesses a Michael acceptor warhead unit and inhibits SARS-CoV-2 3CLpro in the low micromolar range (IC50 = 0.9 µM), was recently demonstrated to exhibit significantly superior antiviral activity in hACE2 cell assays (EC<sub>50</sub> = 8.2 nM). 100 Upon further investigation, this enhanced potency was attributed to a dual mode of action of compound 45 in targeting the SARS-CoV-2 virus lifecycle. In addition to inhibiting 3CL<sup>pro</sup>, 45 was found to also inhibit cathepsin L (CatL), a protease enzyme responsible for cleaving the viral Spike protein, promoting cell entry. Intraperitoneal administration of 45 in SARS-CoV-2 infected transgenic mice also showed to cause reduced viral load in the lungs and enhanced survival rate. In line with the development of inhibitors of other viral proteases, the introduction of an



Representative examples of inhibitors targeting  $3C/3CL^{pro}$  containing a  $P_1$  (S)- $\gamma/\delta$ -lactam isostere

aldehyde C-terminal warhead has also proved effective for the discovery of SARS-CoV-2 3CL<sup>pro</sup> inhibitors (46-48). Structurebased design utilising the crystal structure of SARS-CoV 3CL<sup>pro</sup> gave rise to dipeptide aldehyde 46, which demonstrates good anti-SARS-CoV-2 activity (EC50 = 0.53 nM) and was selected for further preclinical development. 101 Compounds 47 (aka MI-30)<sup>102</sup> and **48** (aka UAWJ9-36-3)<sup>103</sup> represent a series of aldehyde-based hybrid inhibitors which combine the  $P_1(S)$ - $\gamma$ lactam group with a bicycloproline P2 residue derived from the hepatitis C virus (HCV) inhibitors, telaprevir104 (P2 5,5-fused ring) or boceprevir<sup>105</sup> (P<sub>2</sub> 3,5-fused ring), respectively. Unlike work towards other viral 3C/3CL<sup>pro</sup> inhibitors highlighted in this review, SARS-CoV-2 inhibitors are now at various stages of clinical development (Fig. 11). Compound 49 (aka PF-00835231), containing a  $P_1$  (S)- $\gamma$ -lactam group in conjunction with a hydroxymethylketone C-terminal electrophilic warhead, was identified as a potent inhibitor of SARS-CoV-2 3CL<sup>pro</sup> (IC<sub>50</sub> = 4 nM) and was selected as the basis for the development of a protease inhibitor for the treatment of COVID-19.106 One drawback of compound 49 that became apparent during preclinical characterisation was its relatively poor intrinsic aqueous solubility ( $< 0.1 \text{ mg mL}^{-1}$ ), which was insufficient to formulate for intravenous (IV) infusion. Accordingly, IV administration was enabled by utilizing a prodrug strategy, resulting in the phosphate prodrug lufotrelvir (compound 50) which displays vastly superior aqueous solubility of  $> 200 \text{ mg mL}^{-1}$  over a pH range suitable for IV infusion. 107 Lufotrelvir (50) is rapidly converted to the active free hydroxymethyl ketone (PF-00835231, 44) following administration. Work towards development of an orally bioavailable SARS-CoV-2 inhibitor has been undertaken by Owen and co-workers (Pfizer). Again using 49 as a lead compound, several modifications were made in order to reduce the hydrogen bond donor (HBD) count which has been shown to correlate with poor oral bioavailability. 108 Changing the electrophilic warhead from a hydroxymethyl ketone (HMK) to a nitrile group significantly increased its oral bioavailability (Oral F = 1.4% vs. 7.6% for otherwise identical HMK and nitrile inhibitors, respectively). It was also noted that compounds containing a nitrile warhead were less likely to undergo epimerization at the P<sub>1</sub> group during chemical synthesis compared to those equipped with heterocyclic ketone warheads that were also being investigated. 108 Incorporation of a P<sub>2</sub> bicycloproline derivative and N-terminal cap modifications afforded nirmatrelvir (51), which displays superior activity (EC<sub>50</sub> = 74.5 nM) and oral bioavailability (F = 50%) over its predecessor 49  $(EC_{50} = 231 \text{ nM}, \text{ oral } F = 1.4\%).^{109}$ 

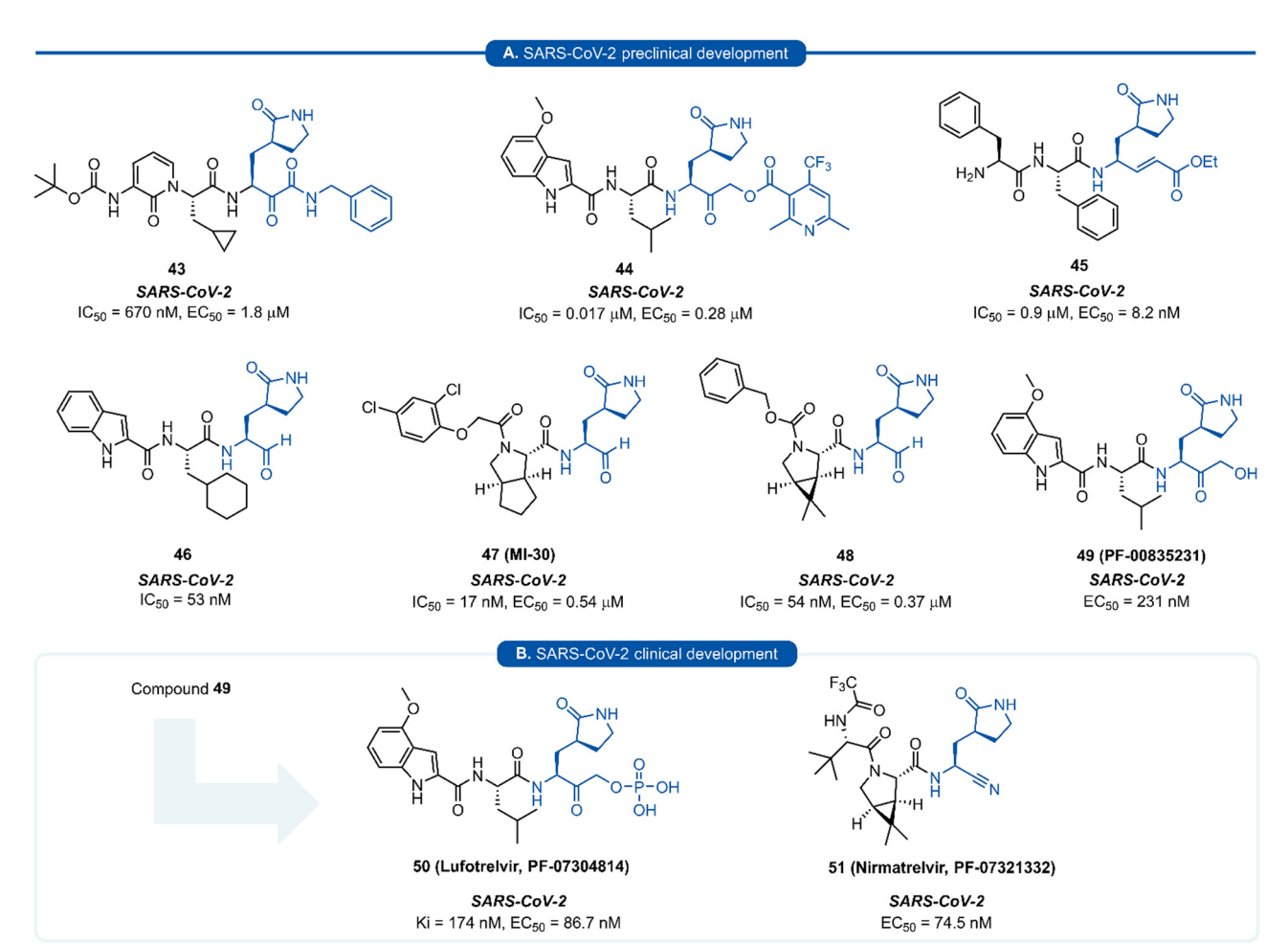
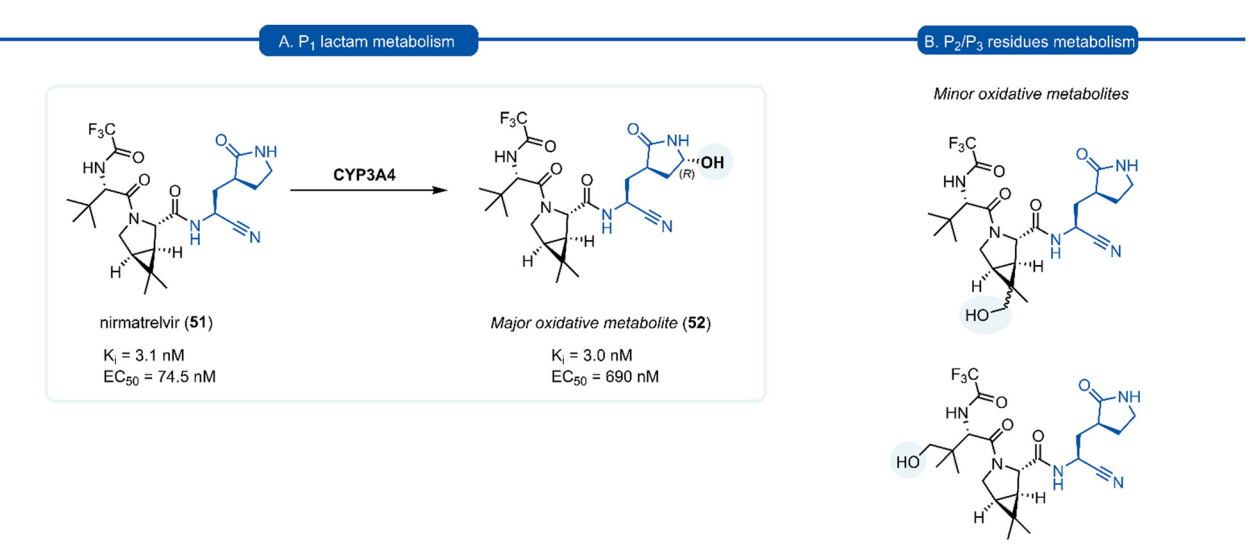


Fig. 11 Representative examples of SARS-CoV-2 inhibitors in preclinical (A) or clinical (B) development.

A drawback of the  $P_1$  (S)- $\gamma$ -lactam glutamine isostere which became apparent through preclinical development of nirmatrelvir (51), is its susceptibility to undergo cytochrome P450

(CYP450) oxidative metabolism. The primary route of inactivation of nirmatrelvir in human liver microsomes occurs via CYP3A4-mediated oxidation. The major metabolite 52 resulting



Scheme 3 (A) The primary route of metabolism of nirmatrelvir 51 via CYP3A4 hydroxylation of the P<sub>1</sub> (S)-γ-lactam moiety. (B) Minor metabolites products of nirmatrelvir 51 via CYP3A4 hydroxylation of the P2 and P3 moiety.

from hydroxylation of the pyrrolidine ring and which, albeit exhibiting similar inhibition potency against 3CL<sup>pro</sup> and repressing viral replication, was 10-fold less active against SARS-CoV-2 compared to 51 in epithelial Vero E6 cells infection model (Scheme 3). In the same study, other minor metabolites of nirmatrelvir, produced by CYP3A4 via alternative oxidation patterns at the  $P_1$  and  $P_2$  position, were detected in trace amounts, but their individual inhibitory potencies were not measured due to their low relative abundance. <sup>109</sup> This has ultimately led to nirmatrelvir being co-administered with the CYP3A4 inhibitor, ritonavir, to increase its bioavailability. This combined formulation, Paxlovid has proven to be a safe and effective treatment for COVID-19 for patients with high risk of disease progression, resulting in an 89% risk reduction in treated patients relative to a placebo group. <sup>110</sup>

# Conclusion

Review

Over the last 25 years, considerable effort has been invested into the development of P<sub>1</sub> glutamine isosteres for incorporation into inhibitors targeting 3C<sup>pro</sup> and 3CL<sup>pro</sup> of viruses in the Pisoniviricetes class. Early efforts exploring P<sub>1</sub> N-alkyl glutamine inhibitors were met with mixed success, while more structurally diverse methionine and carbonyl derived isosteres of glutamine, were generally found to be detrimental to inhibitor activity. Macrocyclization and aza group backbone modifications at the P<sub>1</sub> position, although delivering low micromolar inhibitors, also did not demonstrate any significant improvements over their linear and unmodified counterparts. Incorporation of the P<sub>1</sub> lactam isostere resulted in significantly more potent inhibitors and the development of the (S)- $\gamma$ -lactam moiety marked the first real progress towards potent 3C/3CL<sup>pro</sup> inhibitors. The lactam was found to conformationally restrict the P1 side chain amide bond in the cis conformation, providing optimal H-bonding interactions in the S1 binding pocket and reducing the entropic cost of binding. Moreover, the inhibitor inactivation by intramolecular cyclisation of the nucleophilic P1 amide moiety onto the electrophilic warhead, was not observed for the (S)-lactam. The P1 (S)-lactam moiety has now found widespread use in targeting 3C/3CL<sup>pro</sup> due to its optimal binding interactions and broad compatibility with electrophilic warheads. Recent metabolic studies on nirmatrelvir, however, have now revealed the lactam group to be the primary metabolic hotspot. Although the P1 lactam moiety has provided one of the major milestones in targeting 3Cpro and 3CLpro, further structural optimisation of the lactam side chain is desirable to improve the pharmacokinetics of P<sub>1</sub> lactam containing inhibitors.

# **Author contributions**

L. A. Stubbing: concept and original version. J. Bell-Tyrer: writing – original draft. Y. O. Hermant, J. G. Hubert, S. H. Yang, A. M. McSweeney, G. M. McKenzie-Goldsmith, D. P. Furkert, V. K. Ward, M. A. Brimble: writing – review and editing.

V. K. Ward, M. A. Brimble: project administration, funding acquisition.

# Conflicts of interest

There are no conflicts to declare.

# Acknowledgements

The authors thank the Ministry of Business, Innovation and Employment (MBIE), contract number U00X1904 and Auckland Medical Research Foundation, grant 1720013 for financial support.

# References

- 1 World Health Organization, The top 10 causes of death, https://www.who.int/news-room/fact-sheets/detail/the-top-10-causes-of-death, 2020, accessed 13/03/2023.
- 2 T. Heikkinen and A. Jarvinen, Lancet, 2003, 361, 51.
- 3 X. Wang, J. Ren, Q. Gao, Z. Hu, Y. Sun, X. Li, D. J. Rowlands, W. Yin, J. Wang, D. I. Stuart, Z. Rao and E. E. Fry, *Nature*, 2015, **517**, 85.
- 4 A. Bouin and B. L. Semler, Curr. Clin. Microbiol. Rep., 2020, 7, 31.
- 5 T. M. Szopa, P. A. Titchener, N. D. Portwood and K. W. Taylor, *Diabetologia*, 1993, **36**, 687.
- 6 J. D. Kriesel, A. White, F. G. Hayden, S. L. Spruance and J. Petajan, *Mult. Scler.*, 2004, **10**, 145.
- 7 S. Payne, Viruses, 2017, 149.
- 8 S. M. Ahmed, A. J. Hall, A. E. Robinson, L. Verhoef, P. Premkumar, U. D. Parashar, M. Koopmans and B. A. Lopman, *Lancet Infect. Dis.*, 2014, 14, 725.
- 9 S. C. Baker, *Encyclopedia of Virology*, Oxford Academic Press, Oxford, Third edn, 2008, p. 554.
- 10 D. Sun, S. Chen, A. Cheng and M. Wang, *Viruses*, 2016, 8, 82.
- 11 C. P. Campillay-Veliz, J. J. Carvajal, A. M. Avellaneda, D. Escobar, C. Covian, A. M. Kalergis and M. K. Lay, *Front. Immunol.*, 2020, 11, 961.
- 12 D. A. Matthews, W. W. Smith, R. A. Ferre, B. Condon, G. Budahazi, W. Sisson, J. E. Villafranca, C. A. Janson, H. E. McElroy and C. L. Gribskov, et al., Cell, 1994, 77, 761.
- 13 J. Yin, M. M. Cherney, E. M. Bergmann, J. Zhang, C. Huitema, H. Pettersson, L. D. Eltis, J. C. Vederas and M. N. James, J. Mol. Biol., 2006, 361, 673.
- 14 K. Anand, J. Ziebuhr, P. Wadhwani, J. R. Mesters and R. Hilgenfeld, *Science*, 2003, **300**, 1763.
- 15 X. Fan, X. Li, Y. Zhou, M. Mei, P. Liu, J. Zhao, W. Peng, Z. B. Jiang, S. Yang, B. L. Iverson, G. Zhang and L. Yi, *ACS Chem. Biol.*, 2020, 15, 63.
- 16 H. Chen, Z. Zhu, Y. Qiu, X. Ge, H. Zheng and Y. Peng, Virol. Sin., 2022, 37, 437.

- 17 S. W. Kaldor, M. Hammond, B. A. Dressman, J. M. Labus, F. W. Chadwell, A. D. Kline and B. A. Heinz, Bioorg. Med. Chem. Lett., 1995, 5, 2021.
- 18 P. S. Dragovich, S. E. Webber, R. E. Babine, S. A. Fuhrman, A. K. Patick, D. A. Matthews, C. A. Lee, S. H. Reich, T. J. Prins, J. T. Marakovits, E. S. Littlefield, R. Zhou, J. Tikhe, C. E. Ford, M. B. Wallace, J. W. Meador, 3rd, R. A. Ferre, E. L. Brown, S. L. Binford, J. E. Harr, D. M. DeLisle and S. T. Worland, J. Med. Chem., 1998, 41, 2806.
- 19 P. S. Dragovich, S. E. Webber, R. E. Babine, S. A. Fuhrman, A. K. Patick, D. A. Matthews, S. H. Reich, J. T. Marakovits, T. J. Prins, R. Zhou, J. Tikhe, E. S. Littlefield, T. M. Bleckman, M. B. Wallace, T. L. Little, C. E. Ford, J. W. Meador, 3rd, R. A. Ferre, E. L. Brown, S. L. Binford, D. M. DeLisle and S. T. Worland, J. Med. Chem., 1998, 41, 2819.
- 20 H. Yang, M. Yang, Y. Ding, Y. Liu, Z. Lou, Z. Zhou, L. Sun, L. Mo, S. Ye, H. Pang, G. F. Gao, K. Anand, M. Bartlam, R. Hilgenfeld and Z. Rao, Proc. Natl. Acad. Sci. U. S. A., 2003, 100, 13190.
- 21 P. S. Dragovich, R. Zhou, S. E. Webber, T. J. Prins, A. K. Kwok, K. Okano, S. A. Fuhrman, L. S. Zalman, F. C. Maldonado, E. L. Brown, J. W. Meador, 3rd, A. K. Patick, C. E. Ford, M. A. Brothers, S. L. Binford, D. A. Matthews, R. A. Ferre and S. T. Worland, Bioorg. Med. Chem. Lett., 2000, 10, 45.
- 22 M. A. Murray, J. W. Janc, S. Venkatraman and L. M. Babe, Antivir. Chem. Chemother., 2001, 12, 273.
- 23 M. O. Sydnes, Y. Hayashi, V. K. Sharma, T. Hamada, U. Bacha, J. Barrila, E. Freire and Y. Kiso, Tetrahedron, 2006, 62, 8601.
- 24 S.-H. Chen, J. Lamar, F. Victor, N. Snyder, R. Johnson, B. A. Heinz, M. Wakulchik and Q. M. Wang, Bioorg. Med. Chem. Lett., 2003, 13, 3531.
- 25 M. A. van de Plassche, M. Barniol-Xicota and S. H. Verhelst, ChemBioChem, 2020, 21, 3383.
- 26 C. P. Chuck, C. Chen, Z. Ke, D. C. Wan, H. F. Chow and K. B. Wong, Eur. J. Med. Chem., 2013, 59, 1.
- 27 S. E. Webber, K. Okano, T. L. Little, S. H. Reich, Y. Xin, S. A. Fuhrman, D. A. Matthews, R. A. Love, T. F. Hendrickson, A. K. Patick, J. W. Meador, 3rd, R. A. Ferre, E. L. Brown, C. E. Ford, S. L. Binford and S. T. Worland, J. Med. Chem., 1998, 41, 2786.
- 28 H. Z. Zhang, H. Zhang, W. Kemnitzer, B. Tseng, J. Cinatl, M. Michaelis, H. W. Doerr and S. X. Cai, J. Med. Chem., 2006, 49, 1198.
- 29 B. A. Malcolm, C. Lowe, S. Shechosky, R. T. McKay, C. C. Yang, V. J. Shah, R. J. Simon, J. C. Vederas and D. V. Santi, Biochemistry, 1995, 34, 8172.
- 30 L. S. Deng, Z. Muhaxhiri, M. K. Estes, T. Palzkill, B. V. V. Prasad and Y. C. Song, MedChemComm, 2013, 4, 1354.
- 31 T. S. Morris, S. Frormann, S. Shechosky, C. Lowe, M. S. Lall, V. Gauss-Muller, R. H. Purcell, S. U. Emerson, J. C. Vederas and B. A. Malcolm, *Bioorg. Med. Chem.*, 1997, **5**, 797.

- 32 T. Regnier, D. Sarma, K. Hidaka, U. Bacha, E. Freire, Y. Hayashi and Y. Kiso, Bioorg. Med. Chem. Lett., 2009, 19, 2722.
- 33 Y. K. Ramtohul, M. N. G. James and J. C. Vederas, J. Org. Chem., 2002, 67, 3169.
- 34 T. A. Shepherd, G. A. Cox, E. McKinney, J. Tang, M. Wakulchik, R. E. Zimmerman and E. C. Villarreal, Bioorg. Med. Chem. Lett., 1996, 6, 2893.
- 35 R. D. Hill and J. C. Vederas, J. Org. Chem., 1999, 64, 9538.
- 36 J. S. Kong, S. Venkatraman, K. Furness, S. Nimkar, T. A. Shepherd, Q. M. Wang, J. Aube and R. P. Hanzlik, J. Med. Chem., 1998, 41, 2579.
- 37 Y. M. Shao, W. B. Yang, T. H. Kuo, K. C. Tsai, C. H. Lin, A. S. Yang, P. H. Liang and C. H. Wong, Bioorg. Med. Chem., 2008, 16, 4652.
- 38 L. Li, B. C. Chenna, K. S. Yang, T. R. Cole, Z. T. Goodall, M. Giardini, Z. Moghadamchargari, E. A. Hernandez, J. Gomez, C. M. Calvet, J. A. Bernatchez, D. M. Mellott, J. Zhu, A. Rademacher, D. Thomas, L. R. Blankenship, A. Drelich, A. Laganowsky, C. K. Tseng, W. R. Liu, A. J. Wand, J. Cruz-Reyes, J. L. Siqueira-Neto and T. D. Meek, J. Med. Chem., 2021, 64, 11267.
- 39 J. Zhu, L. Li, A. Drelich, B. C. Chenna, D. M. Mellott, Z. W. Taylor, V. Tat, C. Z. Garcia, A. Katzfuss, C. K. Tseng and T. D. Meek, Front. Chem., 2022, 10, 867928.
- 40 D. H. Goetz, Y. Choe, E. Hansell, Y. T. Chen, M. McDowell, C. B. Jonsson, W. R. Roush, J. McKerrow and C. S. Craik, Biochemistry, 2007, 46, 8744.
- 41 K. Akaji, H. Konno, H. Mitsui, K. Teruya, Y. Shimamoto, Y. Hattori, T. Ozaki, M. Kusunoki and A. Sanjoh, J. Med. Chem., 2011, 54, 7962.
- 42 K. Teruya, Y. Hattori, Y. Shimamoto, K. Kobayashi, A. Sanjoh, A. Nakagawa, E. Yamashita and K. Akaji, Biopolymers, 2016, 106, 391.
- 43 Y. Shimamoto, Y. Hattori, K. Kobayashi, K. Teruya, A. Sanjoh, A. Nakagawa, E. Yamashita and K. Akaji, Bioorg. Med. Chem., 2015, 23, 876.
- 44 K. Ohnishi, Y. Hattori, K. Kobayashi and K. Akaji, Bioorg. Med. Chem., 2019, 27, 425.
- 45 S. Konno, P. Thanigaimalai, T. Yamamoto, K. Nakada, R. Kakiuchi, K. Takayama, Y. Yamazaki, F. Yakushiji, K. Akaji, Y. Kiso, Y. Kawasaki, S. E. Chen, E. Freire and Y. Hayashi, Bioorg. Med. Chem., 2013, 21, 412.
- 46 C. Proulx, D. Sabatino, R. Hopewell, J. Spiegel, Y. Garcia Ramos and W. D. Lubell, Future Med. Chem., 2011, 3, 1139.
- 47 J. Magrath and R. H. Abeles, J. Med. Chem., 1992, 35, 4279.
- 48 S. Venkatraman, J. S. Kong, S. Nimkar, Q. M. Wang, J. Aube and R. P. Hanzlik, Bioorg. Med. Chem. Lett., 1999, 9, 577.
- 49 W. M. Kati, H. L. Sham, J. O. McCall, D. A. Montgomery, G. T. Wang, W. Rosenbrook, L. Miesbauer, A. Buko and D. W. Norbeck, Arch. Biochem. Biophys., 1999, 362, 363.
- 50 H. L. Sham, W. Rosenbrook, W. Kati, D. A. Betebenner, N. E. Wideburg, A. Saldivar, J. J. Plattner and D. W. Norbeck, J. Chem. Soc., Perkin Trans. 1, 1995, 1081.
- 51 Y. T. Huang, B. A. Malcolm and J. C. Vederas, Bioorg. Med. Chem., 1999, 7, 607.

- 52 T. W. Lee, M. M. Cherney, C. Huitema, J. Liu, K. E. James, J. C. Powers, L. D. Eltis and M. N. James, *J. Mol. Biol.*, 2005, 353, 1137.
- 53 T. W. Lee, M. M. Cherney, J. Liu, K. E. James, J. C. Powers, L. D. Eltis and M. N. James, *J. Mol. Biol.*, 2007, 366, 916.
- 54 J. Breidenbach, C. Lemke, T. Pillaiyar, L. Schakel, G. Al Hamwi, M. Diett, R. Gedschold, N. Geiger, V. Lopez, S. Mirza, V. Namasivayam, A. C. Schiedel, K. Sylvester, D. Thimm, C. Vielmuth, L. Phuong Vu, M. Zyulina, J. Bodem, M. Gutschow and C. E. Muller, *Angew. Chem.*, *Int. Ed.*, 2021, 60, 10423.
- 55 C. Gilon, D. Halle, M. Chorev, Z. Selinger and G. Byk, *Biopolymers*, 1991, 31, 745.
- 56 J. D. Tyndall and D. P. Fairlie, Curr. Med. Chem., 2001, 8, 893.
- 57 M. P. Glenn, L. K. Pattenden, R. C. Reid, D. P. Tyssen, J. D. Tyndall, C. J. Birch and D. P. Fairlie, *J. Med. Chem.*, 2002, 45, 371.
- 58 C. J. White and A. K. Yudin, Nat. Chem., 2011, 3, 509.
- 59 E. Marsault and M. L. Peterson, *J. Med. Chem.*, 2011, **54**, 1961.
- 60 F. Giordanetto and J. Kihlberg, J. Med. Chem., 2014, 57, 278.
- 61 S. R. Mandadapu, P. M. Weerawarna, A. M. Prior, R. A. Uy, S. Aravapalli, K. R. Alliston, G. H. Lushington, Y. Kim, D. H. Hua, K. O. Chang and W. C. Groutas, *Bioorg. Med. Chem. Lett.*, 2013, 23, 3709.
- 62 P. M. Weerawarna, Y. Kim, A. C. Galasiti Kankanamalage, V. C. Damalanka, G. H. Lushington, K. R. Alliston, N. Mehzabeen, K. P. Battaile, S. Lovell, K. O. Chang and W. C. Groutas, Eur. J. Med. Chem., 2016, 119, 300.
- 63 A. C. Galasiti Kankanamalage, P. M. Weerawarna, A. D. Rathnayake, Y. Kim, N. Mehzabeen, K. P. Battaile, S. Lovell, K. O. Chang and W. C. Groutas, *Proteins*, 2019, 87, 579.
- 64 V. C. Damalanka, Y. Kim, A. C. Galasiti Kankanamalage, G. H. Lushington, N. Mehzabeen, K. P. Battaile, S. Lovell, K. O. Chang and W. C. Groutas, *Eur. J. Med. Chem.*, 2017, 127, 41.
- 65 K. Namoto, F. Sirockin, H. Sellner, C. Wiesmann, F. Villard, R. J. Moreau, E. Valeur, S. C. Paulding, S. Schleeger, K. Schipp, J. Loup, L. Andrews, R. Swale, M. Robinson and C. J. Farady, *Bioorg. Med. Chem. Lett.*, 2018, 28, 906.
- 66 P. S. Dragovich, T. J. Prins, R. Zhou, S. A. Fuhrman, A. K. Patick, D. A. Matthews, C. E. Ford, J. W. Meador, 3rd, R. A. Ferre and S. T. Worland, *J. Med. Chem.*, 1999, 42, 1203.
- 67 P. S. Dragovich, T. J. Prins, R. Zhou, S. E. Webber, J. T. Marakovits, S. A. Fuhrman, A. K. Patick, D. A. Matthews, C. A. Lee and C. E. Ford, *J. Med. Chem.*, 1999, 42, 1213.
- 68 R. P. Jain and J. C. Vederas, *Bioorg. Med. Chem. Lett.*, 2004, **14**, 3655.
- 69 C. J. Kuo, J. J. Shie, J. M. Fang, G. R. Yen, J. T. A. Hsu, H. G. Liu, S. N. Tseng, S. C. Chang, C. Y. Lee, S. R. Shih and P. H. Liang, *Bioorg. Med. Chem.*, 2008, 16, 7388.

- 70 Y. Wang, B. Yang, Y. Zhai, Z. Yin, Y. Sun and Z. Rao, Antimicrob. Agents Chemother., 2015, 59, 2636.
- 71 Y. Wang, L. Cao, Y. Zhai, Z. Yin, Y. Sun and L. Shang, Antimicrob. Agents Chemother., 2017, 61, e00298.
- 72 Y. Y. Zhai, X. S. Zhao, Z. J. Cui, M. Wang, Y. X. Wang, L. F. Li, Q. Sun, X. Yang, D. B. Zeng, Y. Liu, Y. N. Sun, Z. Y. Lou, L. Q. Shang and Z. Yin, *J. Med. Chem.*, 2015, 58, 9414.
- 73 D. Zeng, Y. Ma, R. Zhang, Q. Nie, Z. Cui, Y. Wang, L. Shang and Z. Yin, *Bioorg. Med. Chem. Lett.*, 2016, 26, 1762.
- 74 Y. Y. Zhai, Y. Y. Ma, F. Ma, Q. D. Nie, X. J. Ren, Y. X. Wang, L. Q. Shang and Z. Yin, *Eur. J. Med. Chem.*, 2016, **124**, 559.
- 75 K. C. Tiew, G. He, S. Aravapalli, S. R. Mandadapu, M. R. Gunnam, K. R. Alliston, G. H. Lushington, Y. Kim, K. O. Chang and W. C. Groutas, *Bioorg. Med. Chem. Lett.*, 2011, 21, 5315.
- 76 A. C. Galasiti Kankanamalage, Y. Kim, P. M. Weerawarna, R. A. Z. Uy, V. C. Damalanka, S. R. Mandadapu, K. R. Alliston, N. Mehzabeen, K. P. Battaile and S. Lovell, *J. Med. Chem.*, 2015, 58, 3144.
- 77 A. D. Rathnayake, Y. Kim, C. S. Dampalla, H. N. Nguyen, A. M. Jesri, M. M. Kashipathy, G. H. Lushington, K. P. Battaile, S. Lovell, K. O. Chang and W. C. Groutas, *J. Med. Chem.*, 2020, 63, 11945.
- 78 A. C. Galasiti Kankanamalage, Y. Kim, A. D. Rathnayake, K. R. Alliston, M. M. Butler, S. C. Cardinale, T. L. Bowlin, W. C. Groutas and K. O. Chang, J. Med. Chem., 2017, 60, 6239.
- 79 F. Amblard, S. M. Zhou, P. Liu, J. Yoon, B. Cox, K. Muzzarelli, B. D. Kuiper, L. C. Kovari and R. F. Schinazi, *Bioorg. Med. Chem. Lett.*, 2018, 28, 2165.
- 80 R. P. Jain, H. I. Pettersson, J. Zhang, K. D. Aull, P. D. Fortin, C. Huitema, L. D. Eltis, J. C. Parrish, M. N. James and D. S. Wishart, J. Med. Chem., 2004, 47, 6113.
- 81 A. K. Ghosh, K. Xi, K. Ratia, B. D. Santarsiero, W. Fu, B. H. Harcourt, P. A. Rota, S. C. Baker, M. E. Johnson and A. D. Mesecar, *J. Med. Chem.*, 2005, **48**, 6767.
- 82 H. Yang, W. Xie, X. Xue, K. Yang, J. Ma, W. Liang, Q. Zhao, Z. Zhou, D. Pei, J. Ziebuhr, R. Hilgenfeld, K. Y. Yuen, L. Wong, G. Gao, S. Chen, Z. Chen, D. Ma, M. Bartlam and Z. Rao, *PLoS Biol.*, 2005, 3, e324.
- 83 S. Yang, S. J. Chen, M. F. Hsu, J. D. Wu, C. T. Tseng, Y. F. Liu, H. C. Chen, C. W. Kuo, C. S. Wu, L. W. Chang, W. C. Chen, S. Y. Liao, T. Y. Chang, H. H. Hung, H. L. Shr, C. Y. Liu, Y. A. Huang, L. Y. Chang, J. C. Hsu, C. J. Peters, A. H. Wang and M. C. Hsu, J. Med. Chem., 2006, 49, 4971.
- 84 P. Thanigaimalai, S. Konno, T. Yamamoto, Y. Koiwai, A. Taguchi, K. Takayama, F. Yakushiji, K. Akaji, S. E. Chen, A. Naser-Tavakolian, A. Schon, E. Freire and Y. Hayashi, Eur. J. Med. Chem., 2013, 68, 372.
- 85 P. Thanigaimalai, S. Konno, T. Yamamoto, Y. Koiwai, A. Taguchi, K. Takayama, F. Yakushiji, K. Akaji, Y. Kiso, Y. Kawasaki, S. E. Chen, A. Naser-Tavakolian, A. Schon, E. Freire and Y. Hayashi, Eur. J. Med. Chem., 2013, 65, 436.
- 86 C. S. B. Chia, W. Xu and P. Shuyi Ng, *ChemMedChem*, 2022, 17, e202100576.
- 87 K. Akaji, Amino Acids Pept. Proteins, 2017, 228.

- 88 T. Pillaiyar, M. Manickam, V. Namasivayam, Y. Hayashi and S. H. Jung, J. Med. Chem., 2016, 59, 6595.
- 89 T. Pillaiyar, L. L. Wendt, M. Manickam and M. Easwaran, Med. Res. Rev., 2021, 41, 72.
- 90 V. Kumar, J. S. Shin, J. J. Shie, K. B. Ku, C. Kim, Y. Y. Go, K. F. Huang, M. Kim and P. H. Liang, Antiviral Res., 2017, **141**, 101.
- 91 A. C. G. Kankanamalage, Y. Kim, V. C. Damalanka, A. D. Rathnayake, A. R. Fehr, N. Mehzabeen, K. P. Battaile, S. Lovell, G. H. Lushington, S. Perlman, K. O. Chang and W. C. Groutas, Eur. J. Med. Chem., 2018, 150, 334.
- 92 L. Zhang, D. Lin, Y. Kusov, Y. Nian, Q. Ma, J. Wang, A. Von Brunn, P. Leyssen, K. Lanko and J. Neyts, J. Med. Chem., 2020, 63, 4562.
- 93 S. L. Binford, F. Maldonado, M. A. Brothers, P. T. Weady, L. S. Zalman, J. W. Meador, 3rd, D. A. Matthews and A. K. Patick, Antimicrob. Agents Chemother., 2005, 49, 619.
- 94 H. M. Wang and P. H. Liang, Expert Opin. Ther. Pat., 2010, 20, 59.
- 95 R. Ramajayam, K. P. Tan and P. H. Liang, Biochem. Soc. Trans., 2011, 39, 1371.
- 96 Y. Kim, S. Lovell, K. C. Tiew, S. R. Mandadapu, K. R. Alliston, K. P. Battaile, W. C. Groutas and K. O. Chang, J. Virol., 2012, 86, 11754.
- 97 J. Tan, K. H. Verschueren, K. Anand, J. Shen, M. Yang, Y. Xu, Z. Rao, J. Bigalke, B. Heisen, J. R. Mesters, K. Chen, X. Shen, H. Jiang and R. Hilgenfeld, J. Mol. Biol., 2005, 354, 25.
- 98 L. Zhang, D. Lin, X. Sun, U. Curth, C. Drosten, L. Sauerhering, S. Becker, K. Rox and R. Hilgenfeld, Science, 2020, 368, 409.
- 99 B. Bai, A. Belovodskiy, M. Hena, A. S. Kandadai, M. A. Joyce, H. A. Saffran, J. A. Shields, M. B. Khan, E. Arutyunova, J. Lu, S. K. Bajwa, D. Hockman, C. Fischer, T. Lamer, W. Vuong, M. J. van Belkum, Z. Gu, F. Lin, Y. Du, J. Xu, M. Rahim, H. S. Young, J. C. Vederas, D. L. Tyrrell, M. J. Lemieux and J. A. Nieman, J. Med. Chem., 2022, 65, 2905.
- 100 S. Mondal, Y. Chen, G. J. Lockbaum, S. Sen, S. Chaudhuri, A. C. Reyes, J. M. Lee, A. N. Kaur, N. Sultana and M. D. Cameron, J. Am. Chem. Soc., 2022, 144, 21035.
- 101 W. Dai, B. Zhang, X. M. Jiang, H. Su, J. Li, Y. Zhao, X. Xie, Z. Jin, J. Peng, F. Liu, C. Li, Y. Li, F. Bai, H. Wang, X. Cheng, X. Cen, S. Hu, X. Yang, J. Wang, X. Liu, G. Xiao, H. Jiang, Z. Rao, L. K. Zhang, Y. Xu, H. Yang and H. Liu, Science, 2020, 368, 1331.
- 102 J. Qiao, Y. S. Li, R. Zeng, F. L. Liu, R. H. Luo, C. Huang, Y. F. Wang, J. Zhang, B. Quan, C. Shen, X. Mao, X. Liu, W. Sun, W. Yang, X. Ni, K. Wang, L. Xu, Z. L. Duan, Q. C. Zou, H. L. Zhang, W. Qu, Y. H. Long, M. H. Li, R. C. Yang, X. Liu, J. You, Y. Zhou, R. Yao, W. P. Li, J. M. Liu, P. Chen, Y. Liu, G. F. Lin, X. Yang, J. Zou, L. Li, Y. Hu, G. W. Lu, W. M. Li, Y. Q. Wei, Y. T. Zheng, J. Lei and S. Yang, Science, 2021, 371, 1374.
- 103 Z. Xia, M. Sacco, Y. Hu, C. Ma, X. Meng, F. Zhang, T. Szeto, Y. Xiang, Y. Chen and J. Wang, ACS Pharmacol. Transl. Sci., 2021, 4, 1408.

- 104 C. Lin, K. Lin, Y. P. Luong, B. G. Rao, Y. Y. Wei, D. L. Brennan, J. R. Fulghum, H. M. Hsiao, S. Ma, J. P. Maxwell, K. M. Cottrell, R. B. Perni, C. A. Gates and A. D. Kwong, J. Biol. Chem., 2004, 279, 17508.
- 105 S. Venkatraman, S. L. Bogen, A. Arasappan, F. Bennett, K. Chen, E. Jao, Y. T. Liu, R. Lovey, S. Hendrata, Y. Huang, W. Pan, T. Parekh, P. Pinto, V. Popov, R. Pike, S. Ruan, B. Santhanam, B. Vibulbhan, W. Wu, W. Yang, J. Kong, X. Liang, J. Wong, R. Liu, N. Butkiewicz, R. Chase, A. Hart, S. Agrawal, P. Ingravallo, J. Pichardo, R. Kong, B. Baroudy, B. Malcolm, Z. Guo, A. Prongay, V. Madison, L. Broske, X. Cui, K. C. Cheng, Y. Hsieh, J. M. Brisson, D. Prelusky, W. Korfmacher, R. White, S. Bogdanowich-Knipp, A. Pavlovsky, P. Bradley, A. K. Saksena, A. Ganguly, J. Piwinski, V. Girijavallabhan and F. G. Njoroge, J. Med. Chem., 2006, 49, 6074.
- 106 R. L. Hoffman, R. S. Kania, M. A. Brothers, J. F. Davies, R. A. Ferre, K. S. Gajiwala, M. He, R. J. Hogan, K. Kozminski, L. Y. Li, J. W. Lockner, J. Lou, M. T. Marra, L. J. Mitchell, Jr., B. W. Murray, J. A. Nieman, S. Noell, S. P. Planken, T. Rowe, K. Ryan, G. J. Smith, 3rd, J. E. Solowiej, C. M. Steppan and B. Taggart, J. Med. Chem., 2020, 63, 12725.
- 107 B. Boras, R. M. Jones, B. J. Anson, D. Arenson, L. Aschenbrenner, M. A. Bakowski, N. Beutler, J. Binder, E. Chen, H. Eng, H. Hammond, J. Hammond, R. E. Haupt, R. Hoffman, E. P. Kadar, R. Kania, E. Kimoto, M. G. Kirkpatrick, L. Lanyon, E. K. Lendy, J. R. Lillis, J. Logue, S. A. Luthra, C. Ma, S. W. Mason, M. E. McGrath, S. Noell, R. S. Obach, O. B. Mn, R. O'Connor, K. Ogilvie, D. Owen, M. Pettersson, M. R. Reese, T. F. Rogers, R. Rosales, M. I. Rossulek, J. G. Sathish, N. Shirai, C. Steppan, M. Ticehurst, L. W. Updyke, S. Weston, Y. Zhu, K. M. White, A. Garcia-Sastre, J. Wang, A. K. Chatterjee, A. D. Mesecar, M. B. Frieman, A. S. Anderson and C. Allerton, Nat. Commun., 2021, 12, 6055.
- 108 D. R. Owen, C. M. N. Allerton, A. S. Anderson, L. Aschenbrenner, M. Avery, S. Berritt, B. Boras, R. D. Cardin, A. Carlo, K. J. Coffman, A. Dantonio, L. Di, H. Eng, R. Ferre, K. S. Gajiwala, S. A. Gibson, S. E. Greasley, B. L. Hurst, E. P. Kadar, A. S. Kalgutkar, J. C. Lee, J. Lee, W. Liu, S. W. Mason, S. Noell, J. J. Novak, R. S. Obach, K. Ogilvie, N. C. Patel, M. Pettersson, D. K. Rai, M. R. Reese, M. F. Sammons, J. G. Sathish, R. S. P. Singh, C. M. Steppan, A. E. Stewart, J. B. Tuttle, L. Updyke, P. R. Verhoest, L. Wei, Q. Yang and Y. Zhu, Science, 2021, 374, 1586.
- 109 H. Eng, A. L. Dantonio, E. P. Kadar, R. S. Obach, L. Di, J. Lin, N. C. Patel, B. Boras, G. S. Walker, J. J. Novak, E. Kimoto, R. S. P. Singh and A. S. Kalgutkar, *Drug Metab*. Dispos., 2022, 50, 576.
- 110 J. Hammond, H. Leister-Tebbe, A. Gardner, P. Abreu, W. Bao, W. Wisemandle, M. Baniecki, V. M. Hendrick, B. Damle, A. Simon-Campos, R. Pypstra, J. M. Rusnak and E.-H. Investigators, N. Engl. J. Med, 2022, 386, 1397.